Comparative Biophysical Studies of Sartan Class Drug Molecules Losartan and Candesartan (CV-11974) with Membrane Bilayers

Charalambos Fotakis,[†,‡] Dionysios Christodouleas,[†,‡] Panagiotis Zoumpoulakis,[†] Eftichia Kritsi,[†,‡] Nikolas-Ploutarch Benetis,[†] Thomas Mavromoustakos,[†,‡] Heribert Reis,[†] Argiro Gili,[†,§] Manthos G. Papadopoulos,[†] and Maria Zervou*,[†]

[†]Institute of Organic and Pharmaceutical Chemistry, National Hellenic Research Foundation, Vas. Constantinou 48, Athens 11635, Greece

[‡]Chemistry Department, National and Kapodistrian University of Athens, Panepistimiopolis Zographou 15771, Greece

[§]School of Applied Mathematical and Physical Science, National Technical University of Athens, Zographou Campus, 15700 Athens, Greece

Ⓢ *Supporting Information*

ABSTRACT: The interactions of the antihypertensive AT_1 antagonists candesartan and losartan with membrane bilayers were studied through the application of DSC, Raman, and solid state ^{31}P NMR spectroscopies. ^1H and ^{13}C NMR resonances of candesartan were assigned on the basis of 1D and 2D NMR spectroscopy. A ^{31}P CP NMR broadline fitting methodology in combination with ab initio computations was implemented and, in conjunction with DSC and Raman results, provided valuable information regarding the perturbation, localization, orienta-

tion, and dynamic properties of the drugs in membrane models. In particular, results indicate that losartan anchors in the mesophase region of the lipid bilayers with the tetrazole group oriented toward the polar headgroup, whereas candesartan has less definite localization spanning from water interface toward the mesophase and upper segment of the hydrophobic region. Both sartan molecules decrease the mobilization of the phospholipids alkyl chains. Losartan exerts stronger interactions compared with candesartan, as depicted by the more prominent thermal, structural, and dipolar $^1H-^{31}P$ changes that are caused in the lipid bilayers. At higher concentrations, candesartan strengthens the polar interactions and induces increased order at the bilayer surface. At the highest concentration used (20 mol %), only losartan induces formation of microdomains attributed to the flexibility of its alkyl chain. These results in correlation to reported data with other AT_1 antagonists strengthen the hypothesis that this class of molecules may approach the active site of the receptor by insertion in the lipid core, followed by lateral diffusion toward the binding site. Further, the similarities and differences of these drugs in their interactions with lipid bilayers establish, at least in part, their pharmacological properties.
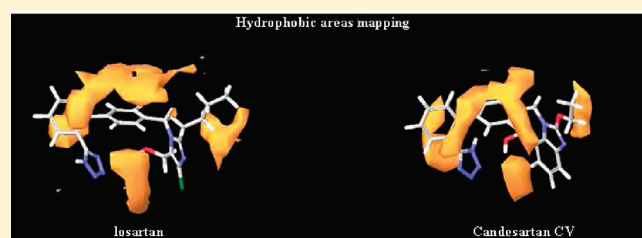
■ INTRODUCTION

Angiotensin II (AngII) receptor antagonists are amphiphilic molecules that exert their biological activity by preventing the vasoconstrictive hormone AngII from acting on the AT_1 receptor, which is a member of the G protein-coupled receptor (GPCR) superfamily.[1]

Losartan (Cozaar) is the first commercially available antihypertensive AT_1 antagonist of the sartans class (Figure 1) and has a proven binding affinity with a competitive/surmountable character of inhibition. Candesartan (CV-11974) is classified as a noncompetitive/insurmountable antagonist and is the active metabolite of candesartan cilexetil (Atacand), which belongs to the sartan class and exerts a longer duration of action showing the highest receptor affinity among the AT_1 sartan antagonists.[2,3] The slow dissociation rate of candesartan probing to differentiated binding properties compared with losartan as well as rebinding mechanism which relates to the retaining of dissociated

ligands within the cell plasma membranes in the neighborhood of receptor molecules could possibly explain its long duration of action. In this context, in vivo experiments and studies in clinical settings appear to indicate that the AT_1 receptor blockade by candesartan is far longer than expected on the basis of the drug plasma concentration.[4] In addition, candesartan has shown a potent inverse agonist profile by means of inhibiting mechanical stress-induced activation of AT_1 receptor (independent of AngII stimulation), which is associated with cardiac hypertrophy.[5] Such an inverse agonist activity has not been shown for losartan. Molecular modeling studies suggest that the binding of candesartan induces distinct conformational changes toward the inactivation of the receptor.[6]
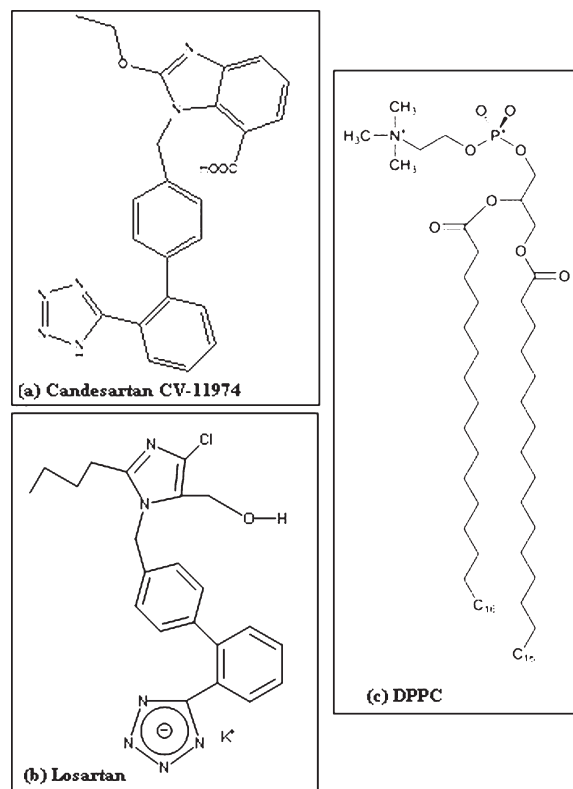
Figure 1. Structures of (a) candesartan, (b) losartan, and (c) DPPC.

On the basis of their amphiphilic profile, a two-step model has been previously reported by the authors in an effort to elucidate the molecular basis of their action.[7] In the first step, the molecules are incorporated into the bilayers through the lipid−water interface, and second, they laterally diffuse to reach the active site of the AT$_1$ receptor to exert their biological activity. The diffusion approach, if the ligand partitions nonspecifically in the plasma membrane, could have an influence on the time needed to reach the receptor and, furthermore, could allow the ligand to adopt a more adequate position, orientation, or conformation necessary for its successful interaction with the binding domains of the receptor.[8]

The cellular membranes are complex entities consisting of various kinds of proteins and lipids as well as cholesterol. Phosphatidylcholines (PCs) are the most abundant lipid species in sarcolemma cardiac membranes. The most frequently found among them are PCs with oleic and linoleic chains, and further (L-α-dipalmitoylphosphatidylcholine) DPPC.[9] Hydrated DPPC lipids are used because they spontaneously form multilamellar bilayers, whereas their mesomorphic changes occur in a convenient temperature range between 25 and 50 °C. Their dynamic and thermotropic properties have been extensively explored,[9−19] and their partition coefficient, especially in the fluid state, resembles that of natural cardiac membranes.[20] Phosphatidylcholine bilayers at low temperatures occur in the gel phase (L$_{\beta'}$) and at higher temperatures in the liquid-crystalline phase (L$_{\alpha}$). The transition is accompanied by several structural changes in the lipid molecules as well as systematic alteration in the bilayer geometry; for example, the *trans/gauche* isomerization taking place in the acyl conformation. The average number of *gauche* conformers indicates the effective fluidity, which depends not only on the temperature, but also on perturbation due to the presence of a drug molecule intercalating between the lipids.

The interactions of the commercially available sartan class of molecules with lipid bilayers have triggered the research interest of our group for the past decade.[21−27] Previously published work includes the application of a novel cross-polarization (CP) ^{31}P NMR simulation methodology to study the possible interdigitation effect of losartan in phospholipid bilayers[28] as well as a combination of small- and wide-angle X-ray diffraction (SWAXS), differential scanning calorimetry (DSC), and Raman spectrosopy to study valsartan/membrane interactions.[29]

Losartan and candesartan, although sharing some common pharmacophore groups (imidazole ring, biphenyl group, and tetrazole moiety), exhibit different pharmacological profiles.[4,30,31] Therefore, it was interesting to investigate and compare their effects in lipid bilayers because they constitute the first step toward their binding to the AT$_1$ receptor. For this purpose, solid state ^{31}P NMR spectroscopy, DSC, and Raman spectroscopy have been applied.

This research activity also implements a CP ^{31}P NMR simulation methodology that elaborates an automated fitting method that utilizes 7 parameters and considers the studied DPPC/water multilamellar bilayers immobilized in the time scale of the NMR experiment. The developed model assumes the lipid molecules perform fast overall rotational diffusion in both the liquid crystalline and in the more organized gel phase. Both phases exhibit long-range orientation order, but the gel phase possesses, in addition, long-range translational order. The latter two properties are intimately related to the concept of the packing quality of the lipids in the bilayer. Overall uniaxial rotations, fluctuations or wobbling of the axis of rotation, internal rotations, and lateral diffusion within the plane of the bilayer are motions of the lipid molecules subjected to the restrictions posed by the anisotropic environment of the bilayer. The detailed theory of the broadline CP ^{31}P NMR simulations of fully hydrated DPPC dispersions in the form of lipid bilayers is outlined in our previous publications.[28,32] Finally, ab initio computations complemented the CP ^{31}P NMR simulation methodology in order to obtain information concerning the chemical shielding (CS) tensor.

■ MATERIAL AND METHODS

Sample Preparation. Candesartan was kindly donated by AstraZeneca. Losartan (potassium salt) was kindly donated by Merck (Whitehouse Station, NJ). L-α-DPPC, (99+%) was purchased from Avanti Polar Lipids Inc. (Alabaster, AL), and spectroscopic grade DMSO and CHCl$_3$ were from Sigma Aldrich (St. Louis, MO). For solution NMR measurements, the candesartan concentration used was 10 mM dissolved in DMSO-d_6. For solid state NMR measurements, appropriate amounts of DPPC with or without losartan or candesartan were dissolved in spectroscopic grade chloroform. The solvent was then evaporated by passing a stream of O$_2$-free nitrogen over the solution at 50 °C, and the residue was placed in a vacuum (0.1 mmHg) for 24 h. To obtain measurements, this dry residue was dispersed in appropriate amounts of bidistilled water by vortexing. The lipid content for the three samples used in the stationary ^{31}P NMR experiments was ~40 mg, and water was dispersed within it (50% w/w). The DPPC/losartan or DPPC/candesartan bilayers contained a 20% mol ratio of drug. For DSC measurements, appropriate amounts of DPPC with or without losartan or candesartan, diluted in chloroform, were mixed, dried under stream of N$_2$, and then stored under vacuum overnight. After dispersing in water (50% w/w), portions of the samples (~5 mg) were sealed in stainless steel capsules obtained from Perkin-Elmer (Norwalk, CT). Identical sample preparation was carried out for the Raman spectroscopy measurements. The amount of sample used was ~40 mg.

B

dx.doi.org/10.1021/jp110371k |*J. Phys. Chem. B* XXXX, XXX, 000–000

Solution NMR Measurements. High resolution (HR)-NMR spectra of Candesartan were recorded on a Varian 600 MHz spectrometer (Palo Alto, CA) at 25 °C. All data were collected using standard Varian pulse sequences. Data processing, including apodization, Fourier transformation, and phasing, were performed using Mnova Suite (Mestrelab Research). ^{1}H–^{1}H DQF-COSY (double quantum filter correlation spectroscopy), ^{1}H–^{13}C HSQC (heteronuclear single quantum coherence) and ^{1}H–^{13}C HMBC (heteronuclear multiple bond correlation) experiments assisted the assignment. ROESY experiment was recorded using a mixing time of 150 ms. Typically, the homonuclear proton spectra were acquired with 4096 data points in t_2, 256–512 t_1 increments, 16–64 scans per increment, and a relaxation delay of 1–1.5 s. The ^{1}H–^{13}C HSQC spectrum was recorded with 1024 data points in t_2, 128 t_1 increments, 16 scans per increment, and a relaxation delay of 1s. The ^{1}H–^{13}C HMBC spectrum was recorded with 4096 data points in t_2, 512 t_1 increments, 64 scans per increment, and a relaxation delay of 1s. The ^{13}C spectral width was 23 000 and 30 000 Hz for the HSQC and HMBC experiments, respectively.

Calculation of Solvent Accessible Surfaces. Molecular modeling and calculation of solvent accessible areas were performed using the MacroModel module (Schrodinger Suite 2010).[33] Losartan and candesartan were subjected to energy minimization using OPLS2005 (optimized potentials for liquid simulations) force field[34] and applying conjugate gradient algorithms and a dielectric constant equal to 45, simulating the amphoteric environment of the membrane bilayers system. QikProp[35] was used to calculate the total solvent accessible surface area (SASA) and its hydrophobic and hydrophilic components (FOSA and FISA, correspondingly). The calculated values provide valuable information regarding the location of the molecules in the hydrated membrane system.

Solid State NMR Measurements. Solid state ^{31}P CP NMR spectra of DPPC, with or without candesartan or losartan, were obtained on a Bruker MSL-400 NMR spectrometer (Rheinstetten, Germany) operating at 161.977 MHz using high-power ^{1}H-decoupling. Each spectrum was an accumulation of 1000 scans. The standard CP pulse sequence of the Bruker library was used with the following acquisition parameters: recycling delay 4 s, contact time 5 ms, acquisition time 1 ms, and $\pi/2$ pulse for proton 7 ms. The contact time was chosen to give optimal spectra after testing at 1, 3, and 5 ms. The temperature range used in the experiments was 25–50 °C. The sample was revolved in a 4-mM rotor at a low frequency of 25 Hz. ^{31}P resonance was referenced to H$_3$PO$_4$ (85% in D$_2$O).

DSC Measurements. Thermal scans were carried out using a Perkin-Elmer DSC-7 calorimeter (Norwalk, CT). All samples were scanned from 10 to 60 °C until identical thermal scans using a scanning rate of 2.5 °C/min. T_m (temperature of the thermal transition maximum), T_{pre} (the maximum of the pretransition temperature), and $T_{m1/2}$ (the full width at half-maximum, fwhm of the phase transition curve) parameters were measured. An empty pan for the baseline and a sample containing double-distilled water were run for the temperature range of 10–60 °C as a reference for the background. This background was subtracted from each thermal scan of the samples. The area under the peak represents the enthalpy change during the transition (ΔH). The mean values of ΔH of three identical scans are tabulated.

Raman Measurements. The Raman spectra were obtained at 4 cm^{-1} resolution from 3500 to 400 cm^{-1} with 2 cm^{-1} intervals using a Perkin-Elmer (Shelton, CT) NIR FT-spectrometer

(Spectrum GX II) equipped with a charge-coupled device detector. The measurements were performed at a temperature range of 27–50 °C. The laser power (Nd:YAG beam at 1064 nm) was kept constant at 400 mW during the experiments. Fifteen hundred scans were accumulated, and backscattering light was collected.

^{31}P CP NMR Simulations. All simulations were obtained imposing Lorentzian spin packets, and the experimental spectra were simulated by automated fitting using the downhill simplex algorithm with a convergence criterion of 0.01.[28] The fitting method computes certain parameters from which the following were used to extract information regarding the interactions of sartan molecules with the DPPC bilayers.

Isotropic Chemical Shift (σ^{iso}/ppm). It is characterized by the chemical shielding tensor, which corresponds to the easily recognized average chemical shift of the ^{31}P broadline and is defined as the trace of

$$\sigma^{iso} = \left(\sigma_{xx} + \sigma_{yy} + \sigma_{zz}\right)/3$$

Inhomogeneous Broadening ($\Delta\sigma$/ppm). This measurable, also called the residual anisotropy of the CS tensor, is related to the internal structure of the polar headgroup and corresponds to the total width of the broadline. It is indirectly correlated to the orientation obtained by the axis of rotation of the lipids with respect to the CS principal frame.

Homogeneous Broadening of Spin Packets or Intrinsic Broadening (brd). The main cause of the homogeneous broadening here is the dipolar ^{1}H–^{31}P interaction of the phosphorus with the neighboring methylene protons and also to a minor extend, the CS-tensor anisotropy.

Collective Tilt Angle (ϑ_{DR}). The angle determined by the director D, the unit normal to the lamellae and the long axis of the phospholipid molecules is called ϑ_{DR}. This angle refers to the collective tilt of the lipids and is related to the long-range orientational order of the bilayer. Thus, ϑ_{DR} is an appropriate parameter for the determination of phase transitions.

The CP Enhancement Parameter (CPe). The CP enhancement of the ^{31}P-nucleus is due to the dipolar coupling to the neighboring alkyl protons. The position and the depth of the minimum in the CP ^{31}P broadline can furthermore give additional details about the magnetic, structural, and dynamical parameters of the phospholipids in the bilayer.

Ab Initio Computations of the Chemical Shielding (CS) Tensor. The DPPC molecule was first optimized at the density functional theory (DFT) level with the B3LYP functional, which is known to provide good geometries[36,37] using the medium-large, all-purpose basis set 6-311G**.[38] The CS tensor components were then computed at different levels of quantum theory—at the uncorrelated restricted Hartree–Fock (RHF) level, at the more accurate low-correlated Møller–Plesset theory of second order (MP2),[39] as well as at the DFT level—employing the B3LYP functional. For the CS tensor calculations, the IGLO III basis set, developed specifically for chemical shift calculations by Kutzelnigg et al.,[40,41] was applied to the PO$_2$(OC–)$_2$ fragment, and the rest of the molecule was described for the RHF and B3LYP calculations by the smaller 3-21G basis set. For the computationally more expensive MP2 calculation, the two long alkyl rests of the optimized geometry were cut down to methyl groups, and the STO-3G basis set, instead of 3-21G, was used for the inactive part. It was confirmed by test calculations

C

dx.doi.org/10.1021/jp110371k |*J. Phys. Chem. B* XXXX, XXX, 000–000

Table 1. Structure Elucidation of Candesartan

atom	^{13}C (ppm)	^{1}H (ppm)	multiplicity
27	14.84	1.36	t
26	66.94	4.507	q
11	46.71	5.61	s
13/17	126.86	6.908	d
14/16	129.42	6.99	d
9	121.14	7.16	t
19		7.48	m
22	131.06	7.60	m
8	123.90	7.50	m
21	128.21	7.52	m
20	131.5	7.60	m
10	121.88	7.63	d
7	117.02		
5	131.65		
12	137.18		
15	138.54		
18, 23	141.37		
4, 24	142.05		
2	158.67		
6	167.92		
7	117.02		

that the effect of increasing the part described by IGLO-III, as well as the change of basis sets used for the inactive part of the molecule, had only little effect on the CS tensor.

All computations were performed using Gaussian98.[42] The raw CS tensor obtained from the computations was not completely symmetrical, due in part to calculation inaccuracies but also on theoretical grounds.[43] Following the usual practice, the small antisymmetrical part was disregarded. The principal frame of the CS tensor was determined by diagonalizing the symmetric part of the CS tensor employing standard techniques. The relative isotropic chemical shift, as measured in the NMR experiments, was estimated by calculating additionally the CS tensor of H_3PO_4, which was then used as a reference value, thus simulating the experimental procedure. The geometry of phosphoric acid was optimized at the B3LYP/6-311G** level. For the CS tensor, the IGLO-III basis set was employed to be used as a reference value for the CS tensor of DPPC computed at a specific level of theory (RHF, MP2, B3LYP). The CS tensor of H_3PO4 was computed at the same level of theory as the corresponding calculation of DPPC.

■ RESULTS

Candesartan HR-NMR Profile. Candesartan was dissolved in DMSO solvent that provides an amphiphilic environment reported to mimic the physiological environment of membrane bilayers.[44] The drug structure identification has been assisted by previous reported work with other AT_1 antagonists and synthetic analogues.[23,25,45] 2D homonuclear DQF-COSY and ROESY spectra provided unambiguous assignment of the ^1H resonance peaks. Verification of the carbon chemical shifts was obtained through 2D heteronuclear HSQC and HMBC spectra. Both ^1H and ^{13}C assignments are shown in Table 1. Figure 2A and B depicts the ^1H and ^{13}C NMR spectrum of candesartan.

Solvent-Accessible Surface Areas of Losartan and Candesartan. Calculations of the solvent accessible area for the two molecules are provided in Table 2. The calculation resulted in several values for each parameter. This is due to the different possible tautomers generated for each structure that lead to slightly different conformations that determine the estimation of the properties. Results show that although both losartan and candesartan have similar total SASA, losartan's hydrophobic component FOSA is higher than the corresponding one for candesartan, irrelevantly of their tautomerism. This higher hydrophobic accessible area of losartan may cause repellent interactions from the water molecules. These interactions can be the driving force guiding the molecule deeper spanning the polar headgroup, the mesophase, and the upper segment of hydrocarbon chains of the membranes.

Differential Scanning Calorimetry. Thermal changes in the pure DPPC/water system as well as the influence of increasing molar fraction of either candesartan or losartan in DPPC bilayers are shown in Figure 3. The DSC thermal scans of DPPC/losartan dispersions have already been presented in our previous work,[7] but to directly compare them with the DPPC/candesartan dispersions using the same phospholipid branch and identical equilibration conditions, they were rerun. In Table 3, the main calorimetric parameters describing the interactions of candesartan with DPPC are contrasted with the respective ones of losartan.

In pure DPPC bilayers (top curve), two characteristic endothermic peaks are visible, referring to the pre- and the main transition. Below the pretransition, the DPPC molecules occur in the well organized lamellar gel phase, $L_{\beta'}$, and above the main transition temperature, the fluid lamellar phase, L_α, is formed. An intermediate phase, $P_{\beta'}$, is also observed, in which the bilayers are modulated by a periodic ripple (ripple phase). The recorded transition temperatures and enthalpies are in good agreement with literature values (Table 3).[46]

The insertion of candesartan at increasing concentrations (1, 5, and 20 mol %) suppresses but does not abolish the pretransition peak and lowers the pretransition enthalpy, thus probing only slight interactions with the headgroup. On the other hand, losartan already from 1% mol almost suppresses the pretransition and lowers the enthalpy change. Furthermore, with increasing drug concentration to 5 mol %, the pretransition peak is abolished. This indicates that losartan perturbs more effectively the headgroup region compared with candesartan.[7,47,48]

The T_m of the phase transition is lowered only at 20 mol % incorporated candesartan. In contrast, the insertion of losartan, even at low concentrations, causes a lowering of the phase transition, but a more prominent decrease is observed as the concentration increases. This demonstrates that as their concentration in the bilayer increases, sartans increasingly affect the alkyl chain packing.

The co-operativity (as is reflected by changes of the fwhm of the gel to liquid phase transitions, $T_{m1/2}$) increased slightly with the insertion of candesartan while the incorporation of losartan caused significant increase. Specifically, the extensively broadened peak that is reported as split[7] or not split[47] at 20 mol % of losartan contains more components and is very sensitive to experimental conditions. Consequently, the appearance of different thermal profiles, especially when the drug is incorporated at high concentration, is on one hand attributed to different equilibration conditions, as already discussed in our previous publication,[49] and on the other hand on the basis of its inhomogenous distribution to the bilayers.[7,28,47,48,50]
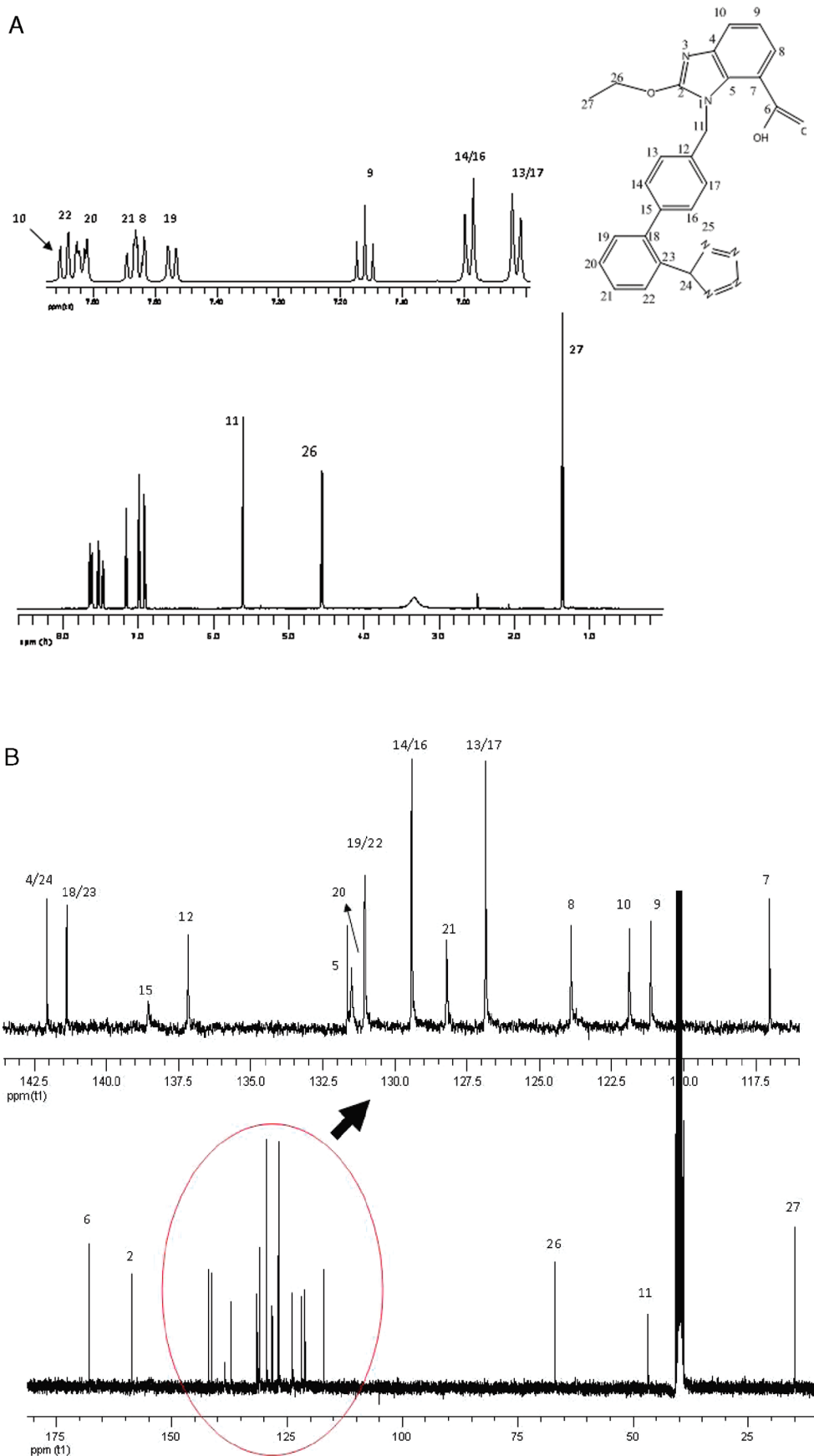
D

dx.doi.org/10.1021/jp110371k |*J. Phys. Chem. B* XXXX, XXX, 000–000

A

B

Figure 2. ^{1}H and ^{13}C NMR spectra of candesartan in DMSO-d_6 solvent at ambient temperature.

Table 2. Calculations of the Solvent-Accessible Area for the Two Molecules[a]

molecule	SASA (Å²)	FOSA (Å²)	FISA (Å²)
losartan	699−710	219−243	129−174
candesartan	674−720	162−165	150−154

[a] SASA, total solvent accessible surface area; FOSA, hydrophobic component of SASA; FISA, hydrophilic component of SASA
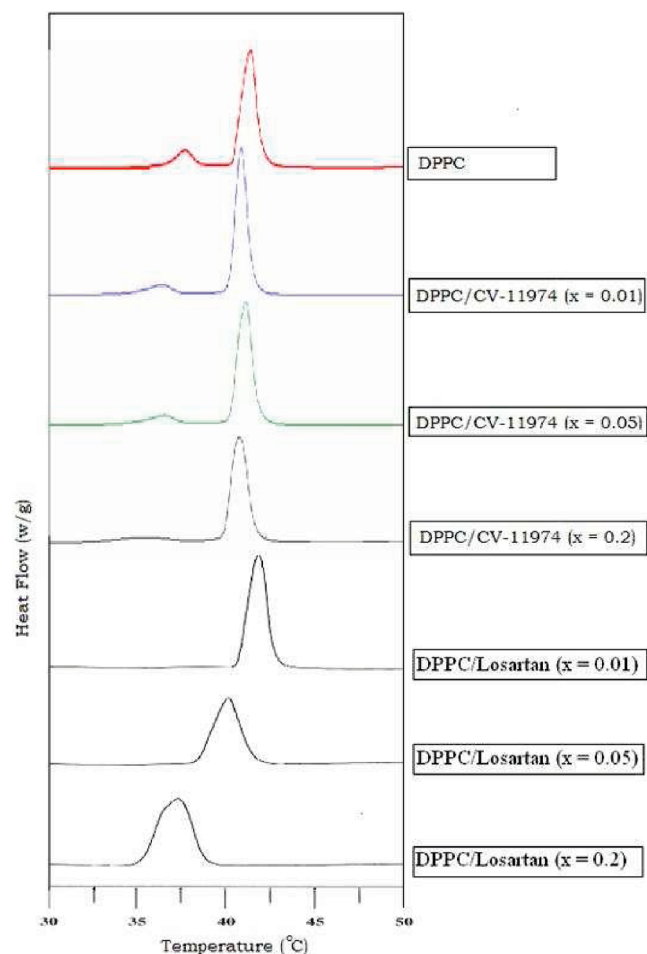
Figure 3. DSC scans of DPPC bilayers containing candesartan and losartan at molar ratios x = 0.01, 0.05, and 0.20.

Notably, an increase in ΔH was observed only with the inclusion of 20% mol losartan, whereas the insertion of 20% mol candesartan did not affect ΔH significantly. It must be clarified that ΔH by itself is not a diagnostic parameter of interdigitation. However, this information can be combined and complemented with different spectroscopy methodologies, such as Raman, solid state NMR, and X-ray diffraction, to prove interdigitation. As we have pointed out in our previous publication, DSC as an easily accessible thermodynamic technique can be applied as the first step in exploring the possibility of interdigitation. The detection of the ΔH increase associated with the incorporation of a drug in the lipid matrix can then be used as a diagnostic parameter to signify partial interdigitation of the lipid bilayers.[50] Recently, we have shown that valsartan increases both the ΔH and *trans/gauche* ratio while it decreases *d*-spacing. All these concomitant events point out that valsartan causes interdigitation in the lipid bilayers.[29]

Table 3. The Calorimetric Parameters, The Pretransition and the Main Transition Temperatures (T_{pre} and T_m respectively), the Half-Width of the Main Transition Peak ($T_{m1/2}$), and the Enthalpy Changes ΔH Associated with the Phase Transitions of DPPC Bilayers Alone and with Incorporated Candesartan or Losartan at Molar Ratios x = 0.01, 0.05 and 0.20

sample	drug concn	ΔH (J/g) pretransition	ΔH (J/g) main transition	$T_{m1/2}$	T_m pretransition	T_m main transition
DPPC		6.82	44.97	1.00	37.67	41.46
candesartan	x = 0.01	5.73	46.66	0.83	36.42	40.92
	x = 0.05	5.64	46.94	1.08	36.5	41.21
	x = 0.2	4.61	44.31	1.17	35.25	40.83
losartan	x = 0.01	1.20	43.70	1.40	27.90	40.70
	x = 0.05		44.10	1.80		38.90
	x = 0.2		55.70	2.00		36.00

Raman Spectroscopy. Raman spectra of pure DPPC bilayers in the presence of x = 0.20 candesartan or losartan were obtained in a temperature range of 27−50 °C. The transition behavior was especially characterized by the C−H and C−C stretching modes. The C−C stretching mode region in the 1050−1150 cm^{-1} spectral interval reflects directly intramolecular *trans/gauche* conformational changes within the hydrocarbon chain region of the lipid matrix. Especially, the temperature profiles of the peak height intensity ratio $I_{1090/1130}$ allow direct comparison of the bilayers' disorder−order characteristics between bilayer preparations without or with drug incorporation.[16,17]

Figure 4 shows the changes in the $I_{1090/1130}$ intensity ratio caused by sartans when incorporated in DPPC bilayers, and the transition temperatures compare well with the results found from the calorimetric measurement. Candesartan and losartan induce lowering of the gauche/trans ratio, as can be observed in Figure 4B and C across the gel-to-fluid-phase transition, since ΔI drops from 0.83 in unloaded DPPC bilayers to about 0.4 and 0.3 for candesartan and losartan, respectively. This signifies that lipid chains in the fluid chain region exhibit fewer *gauche*-to-*trans* isomerizations in the case of bilayers containing candesartan or losartan. In particular, Raman results showed that the gel phase in the presence of sartans appeared more fluid, and the liquid phase, less fluid, in comparison with DPPC bilayers alone. Such behavior is well-known to be exerted by sterols.[51,52]

The *trans/gauche* isomerization reduction points out that the enthalpy increase observed in DSC experiments in the case of losartan is solely attributed to the increase of van der Waals interactions, giving a hint of partial interdigitation effect.[28]

The intermolecular acyl chain interactions of the lipids in the bilayers can be elicited from the 2935/2880 intensity ratio that measures the effects originating from changes both in interchain and intrachain order−disorder processes in the bilayer acyl chains. The band height intensity 2935/2880 ratio constitutes a sensitive probe to monitor the lipid phase transitions, despite the fact that the C−H stretching mode region consists of many superimposed vibrational transitions.[19,53,54] Figure 5 shows changes in the 2935/2880 peak height intensity ratio caused by either losartan or candesartan when they are incorporated in DPPC bilayers. The presence of either sartan lowers ΔI as compared with DPPC bilayers alone during the gel-to-fluid phase transition, indicating a decrease in chain mobility. The effect of candesartan was higher when compared with losartan, attributed probably to the fact that it bears a more rigid heterocyclic segment.
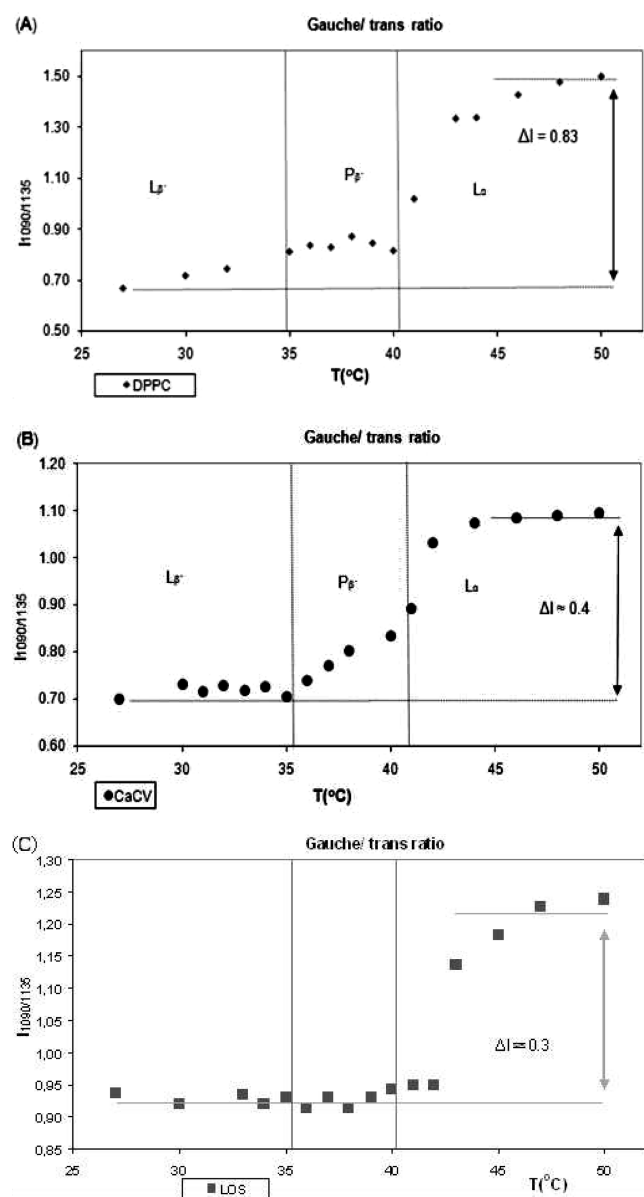
Figure 4. Raman band ratio $I_{1090/1130}$-vs-temperature graphs for (A) DPPC alone, (B) DPPC bilayers containing $x = 0.20$ of candesartan, and (C) DPPC bilayers containing $x = 0.20$ of losartan.
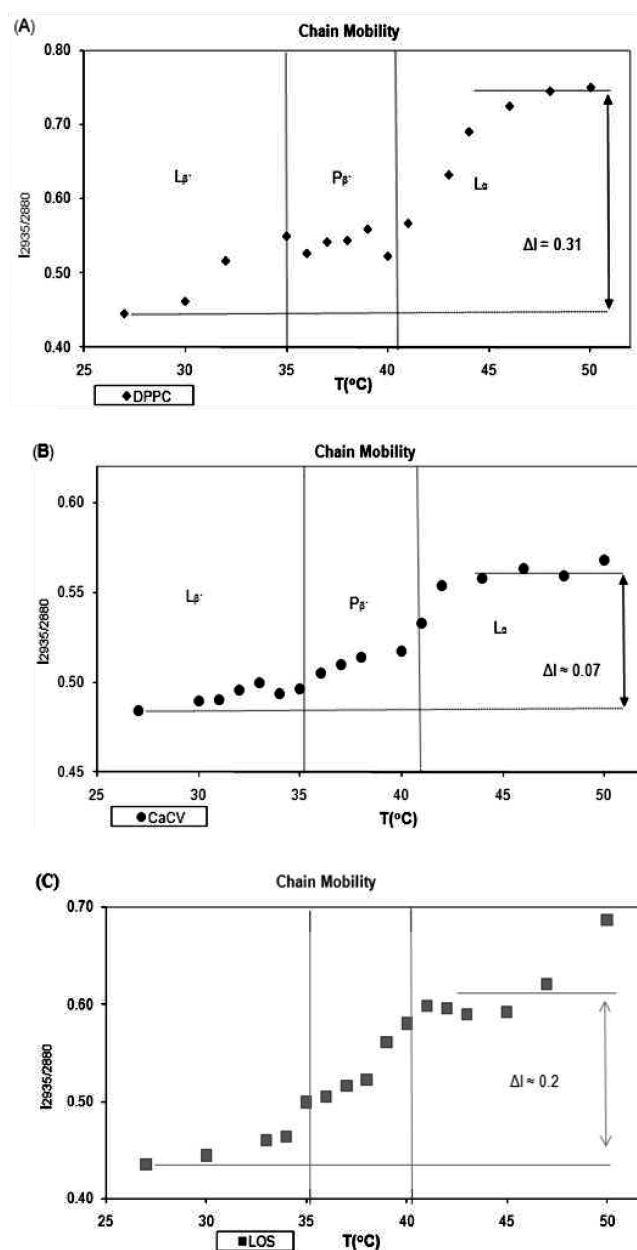

Figure 5. Raman band ratio $I_{2935/2880}$-vs-temperature graphs for (A) DPPC alone and (B) DPPC bilayers containing $x = 0.20$ of candesartan and (C) DPPC bilayers containing $x = 0.20$ of losartan.

Raman results proved the direct incorporation of the two molecules as more peaks attributed solely to aromatic rings or carbonyl groups of the AT$_1$ antagonists appeared in the spectra. At 714 cm^{-1}, corresponding to C–N stretch vibration, a shift to higher values was observed when either candesartan or losartan was incorporated in the membrane bilayers, signifying that both AT$_1$ antagonists interact with the headgroups. This gives also evidence for the strong electrostatic interactions between the negatively charged pharmacophore segments of the AT$_1$ antagonists (tetrazole and carboxylate) and the positively charged choline group. Losartan caused a stronger shift and line-shape changes at 1294 cm^{-1} than candesartan. New peaks due to the presence of candesartan have been observed, resonated at 3070, 1610, and 800 cm^{-1} and attributed to CH aromatic, C=C, and p-substituted benzene vibration stretch, respectively (Supporting Information).

Spectral Simulations of ^{31}P NMR Broadlines. Experimental and simulated spectra of DPPC and DPPC loaded with cadersartan bilayers have been obtained in the temperature range of 25–50 °C and have been compared with the corresponding spectra for losartan presented in our previous publication.[28] Figure 6 presents five representative temperatures that cover all mesomorphic states of the lipid bilayers (25, 30, 35, 40, 45 °C). Figure 6A depicts the lineshapes for the DPPC alone and Figure 6B and C, the dispersions with candesartan and losartan, respectively. Several conclusions can be driven by studying the experimental and simulated spectra. More specifically, the presence of the drug in the lipid bilayers results in (a) modifying the chemical shift toward lower values; (b) the abolishment of the deep minimum observed in the ^{31}P NMR broadline spectra observed, even from the gel phase; and
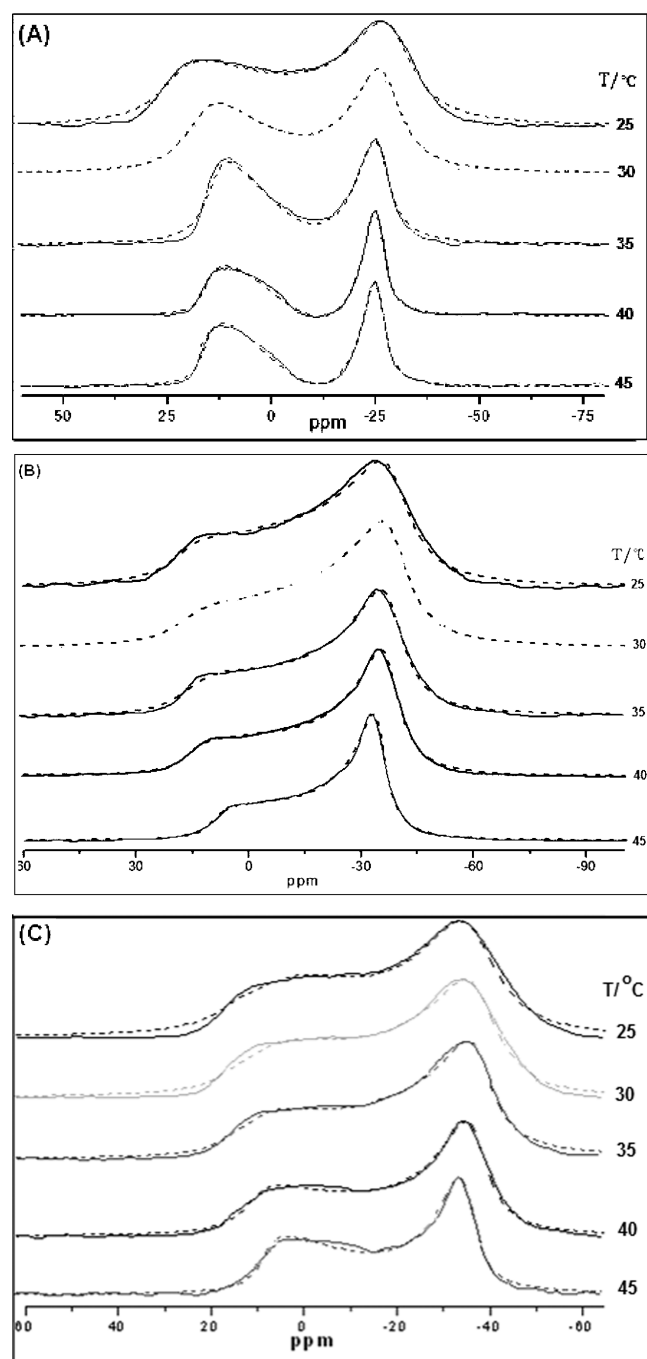
G

dx.doi.org/10.1021/jp110371k |*J. Phys. Chem. B* XXXX, XXX, 000–000

Figure 6. Experimental and simulated ^{31}P CP NMR spectra of DPPC bilayers alone (A), loaded with candesartan at molar ratio $x = 0.20$ (B), and loaded with losartan at molar ratio $x = 0.20$ (C) in the temperature range of 25–50 °C.

Table 4. Spectral Simulation Parameters for CP ^{31}P NMR Spectra of the DPPC Bilayers Alone and with Incorporated Candesartan or Losartan in the Temperature Range 25–50 °C

T °C	brd	σ_{iso}	$\Delta\sigma$	Cpe	ϑ_{DR}
		A: DPPC Bilayers Alone			
25	6.61	−10.55	55.70	0.64	24.64
27	6.83	−10.69	55.17	0.70	29.2
30	5.34	−11.61	47.26	0.87	19.09
32	3.74	−11.71	42.12	0.86	20.53
33	3.32	−12.28	41.6	0.91	16.31
35	2.66	−12.27	41.34	1.03	9.32
36	2.50	−12.08	42.21	1.05	15.82
38	2.24	−12.15	41.55	1.10	3.82
40	1.99	−11.90	41.36	1.06	2.17
42	2.39	−12.03	41.12	1.08	2.78
43	2.30	−12.03	41.10	1.07	4.39
45	2.65	−11.59	41.75	1.11	10.11
46	2.28	−11.62	41.65	1.06	10.24
47	2.09	−11.56	42.11	1.06	11.22
49	2.29	−11.88	42.24	1.13	12.16
50	2.06	−11.76	40.74	1.07	11.51
		B: Containing $x = 0.20$ Candesartan			
25	6.54	−19.47	60.71	0.08	19.50
27	6.30	−19.63	58.37	0.19	22.96
30	6.08	−20.18	58.02	0.13	18.56
32	6.27	−20.56	56.69	0.24	18.12
33	5.59	−20.09	57.87	0.22	18.77
35	5.59	−20.09	57.87	0.22	18.77
36	4.53	−20.32	58.34	0.13	20.43
38	4.37	−20.03	56.04	0.18	14.53
40	4.24	−20.11	53.48	0.29	8.79
42	3.18	−19.26	52.88	0.16	4.91
43	3.09	−19.61	44.97	0.20	6.14
45	3.00	−20.23	44.57	0.31	5.61
46	2.97	−19.87	44.14	0.25	5.87
49	2.91	−20.04	44.55	0.32	5.40
50	2.93	−20.28	44.37	0.33	5.05
		C: Containing $x = 0.20$ Losartan			
25	8.12	−19.93	53.02	0.69	34.15
27	7.35	−19.61	54.58	0.66	35.89
30	6.87	−19.43	55.86	0.57	38.04
32	5.99	−19.88	56.48	0.44	31.98
33	6.08	−20.39	55.47	0.39	30.07
35	5.57	−21.28	54.47	0.27	17.61
36	5.34	−21.87	52.09	0.29	14.09
38	4.93	−21.58	52.11	0.32	13.57
40	4.42	−21.89	52.03	0.28	12.78
42	4.13	−21.68	51.31	0.43	11.06
43	4.22	−21.45	49.98	0.52	17.51
45	3.86	−21.69	47.43	0.61	18.57
46	3.47	−21.57	45.64	0.62	16.83
47	3.33	−21.44	44.05	0.63	14.13
49	2.74	−21.67	42.66	0.67	14.52
50	2.55	−21.72	42.19	0.53	15.19

(c) substantial change of the profile of the spectrum as a function of the temperature.

The spectral simulation parameters of unloaded and loaded DPPC bilayers in the range of 25–50 °C are presented in Table 4. The σ_{iso} and brd temperature profiles can provide information on the sartan localization in the DPPC bilayers due to the drug/membrane interactions. In particular, as presented in Figure 7, the incorporation of a sartan molecule in the bilayers significantly decreases the isotropic chemical shift due to the

extra shielding provided to the ^{31}P bilayer polar head. This indicates that sartan molecules localize in the hydrophilic zone of the phospholipid bilayer formed by the polar headgroups and the lipid–water interface; thus, most probably, the studied sartans bind to the headgroup with the negatively charged groups (tetrazole ring, carboxyl group, or both). The σ_{iso} of DPPC depicts two phases: the first is up to 33 °C, and the second is from 33 up to 50 °C. Losartan insertion lowers the σ_{iso} values more than the candesartan in the latter temperature range, indicating a stronger interaction of losartan with the polar headgroup with respect to candesartan, at least in the liquid crystalline phase.
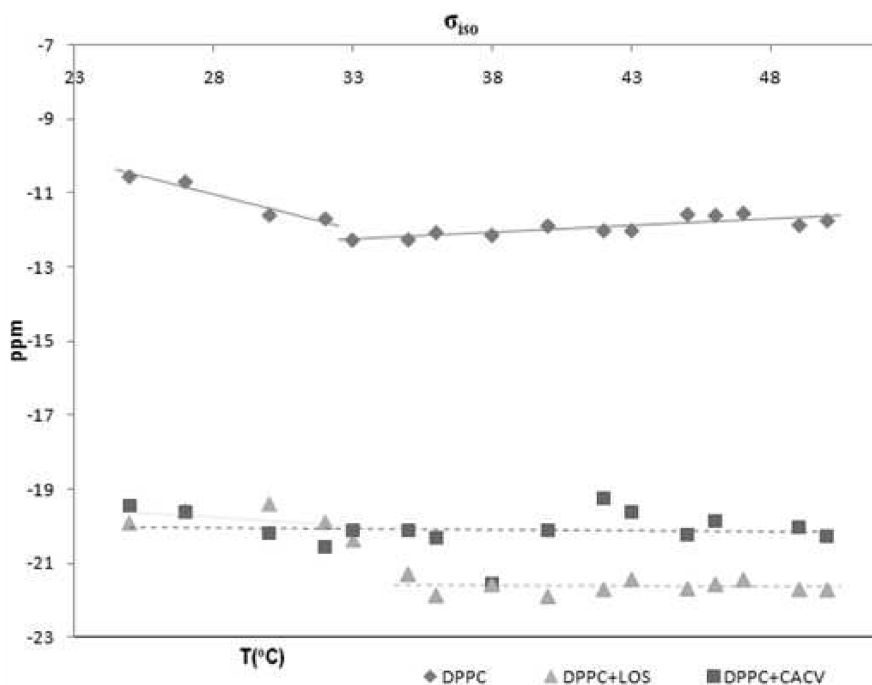
Figure 7. Temperature profiles of the isotropic chemical shift σ_{iso} of the DPPC bilayers without and with candesartan or losartan.
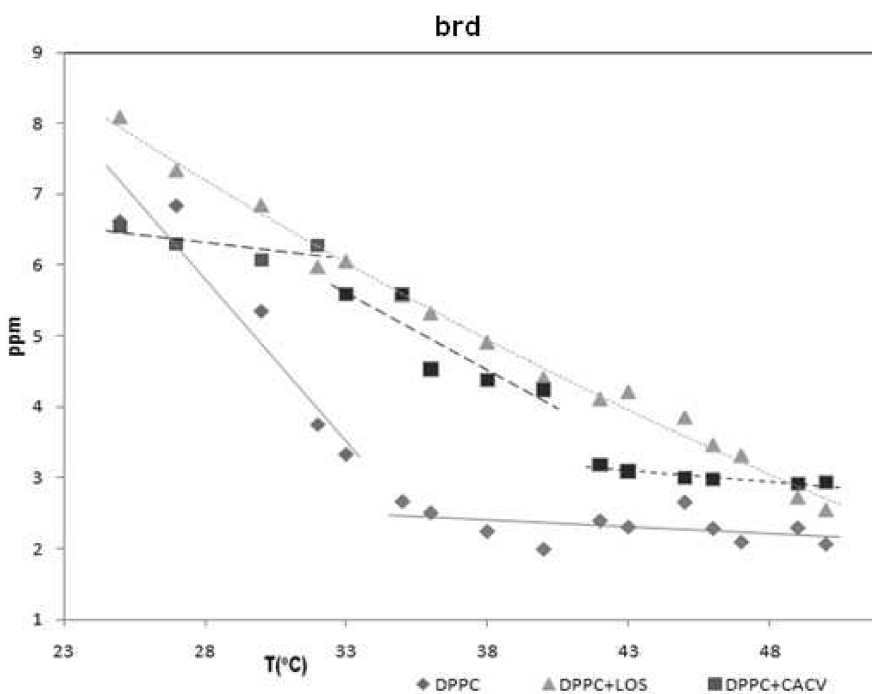

Figure 8. Temperature profiles of the homogeneous broadening of spin packets brd of the DPPC bilayers without and with candesartan or losartan.

The value of this parameter for both free or sartan loaded bilayers is weakly dependent on the temperature.

The brd of unloaded bilayers, as depicted in Figure 8, decreases monotonically in the temperature range 25—33 °C, meaning a higher mobility of the bilayer with the increase in the temperature. The values of brd in sartan loaded bilayers are, in general, higher, deducing that the incorporation of either of these sartans inhibits the bilayer's mobility. The decreased mobility of the bilayers containing sartans with respect to the DPPC bilayers alone show that the drugs are localized close to the polar head moiety and affect the dipolar $^1\mathrm{H}-^{31}\mathrm{P}$ interaction of the phosphorus with the neighboring methylene protons. In the case of losartan, the brd temperature profile is phase-independent, and the brd values are continuously decreasing, reaching the brd values of the unloaded bilayers at 48—50 °C. The lower brd values of candesartan loaded bilayers postulate

I

dx.doi.org/10.1021/jp110371k |*J. Phys. Chem. B* XXXX, XXX, 000–000

Table 5. Ab Initio Values of the Isotropic Chemical Shift As Well As the Principal Components of the Traceless Chemical Shielding Tensor Diagonal of the ^{31}P Nucleus in DPPC and Comparison with the Experimental Values^a

method	σ^{iso}	$\sigma^{ref}-\sigma^{iso b}$	principal components	$\sigma_X-\sigma_Y$	$\sigma_\perp-\sigma_\parallel$
B3LYP	299.17	4.0	−118.6, −69.7, 188.3	−48.9	282.5
RHF	356.08	5.9	−108.0, −64.4, 172.3	−43.6	258.5
RHF^c	355.80	6.2	−107.7, −64.1, 172.6	−43.6	258.5
MP2^c	338.92	6.5	−111.7, −61.6, 173,4	−50.1	260.1
exptl[55]		2.0	(−81.0, −21.0, 108.0)	−60.0	159.0

^{a} All values in ppm. ^{b} Ref = H$_3$PO$_4$, σ^{ref} (RHF) = 361.97 ppm, σ^{ref} (MP2) = 345.42 ppm, σ^{ref} (B3LYP) = 303.14 ppm. ^{c} Fragment with −CH$_3$ instead of the −C$_{15}$H$_{21}$ chains.

weaker dipolar ^{1}H−^{31}P interactions than that of losartan, are phase-dependent, and probe to the phase transitions.

The variations in the collective tilt ϑ_{DR} and the inhomogenous broadening $\Delta\sigma$ parameters as a function of temperature provide information regarding dynamical and conformational characteristics of the bilayers that are affected by the incorporation of the drug. The incorporation of either sartan molecule differentiates their trend with respect to the unloaded bilayers, indicating that the drug molecules disturb the spatial arrangement of the headgroup, but to a different degree. Furthermore, the values of residual anisotropy $\Delta\sigma$ and collective tilt ϑ_{DR} for unloaded and loaded bilayers show that these parameters are phase-dependent. The phase transition from the gel phase to the liquid crystalline phase is accompanied with major rearrangement of the headgroup; thus, the values of these parameters are higher in the gel phase (25−35 °C) and lower in the liquid crystalline phase (43−50 °C).

Ab Initio Computations of the Chemical Shielding (CS) Tensor. In our previous publication,[28] we applied as initial values for the components of the ^{31}P CS tensor in the simulation procedure, the experimental reported data of DPPC dispersions (50 wt % H$_2$O) referenced to 85% H$_3$PO$_4$ at −110 °C.[55] In this research work, we additionally performed ab initio calculations of the CS tensor of DPPC as displayed in Table 5. All the theoretical calculations are able to reproduce the experimental relative isotropic shift. The individual principal components of the traceless shielding tensor and the calculated anisotropy parameters $\sigma_X-\sigma_Y$ and $\sigma_\perp-\sigma_\parallel$ deviate from the reported experimental values.[55] Possible reasons for this disagreement are derived from the fact that computations are performed in isolated molecules of DPPC, whereas the experiments are performed on phospholipid bilayers, which means that not all the environmental effects on a molecule in the phase (local field, confinement effects on geometry, etc.) are taken into account. In addition, only one configuration at the optimum geometry and zero temperature have been considered in the calculation, thus ignoring all the configurational space available to the molecules at the finite temperature at which the experiments were performed. The isotropic chemical shift is an average value and, thus, may not be sensitive to these factors.

■ DISCUSSION

Topography and Interdigitation Effect of the Sartans in Lipid Bilayers. Similarities and differences are observed on the interactions of the two sartan molecules with lipid bilayers. Losartan is administered as a potassium salt, and this may explain

its stronger polar interactions as they are depicted with solid state ^{31}P NMR spectroscopy and DSC.

The inhibition of the pretransition, the lowering of T_m, the shift of the 714 cm^{-1} peak of Raman spectra to higher values, and the decrease in the σ_{iso} value constitute a significant experimental evidence for the sartan molecules' polar interface activity. On the other hand, the more pronounced perturbing effects are exerted by losartan, as it is depicted by (i) the abolishment of pretransition; (ii) the stronger lowering of the main phase transition and (iii) the σ_{iso} value, probe to a different affinity profile for each sartan in the DPPC bilayer core and water interface.

At the given experimental conditions (pH ∼ 7), both the acidic tetrazole and carboxylate groups of candesartan are mostly deprotonized (pK_a ∼ 6 for the terazole ring and pK_a ∼ 3−4 for the carboxylic acid).[56] Losartan features only the acidic group of tetrazole with a negative charge due to its potassium salt form. DPPC is a neutral zwitterionic molecule at physiological pH values bearing the positively charged headgroup choline and the negatively charged phosphate moiety. It is anticipated that the two agents would exhibit different electrostatic interactions with the bilayer interface due to the difference in their negative charges, implying a differentiated affinity to the membrane surface as well as a different immersion of the drugs in the model membranes.

The ϑ_{DR} values of DPPC containing losartan were higher compared with those containing candesartan. This may be related to the topography and the strength of the sartan molecules' binding forces with the lipid bilayers. Experimental results have shown that losartan is localized at the interface that covers the polar region and upper segment of the lipophilic region to maximize its amphipathic interactions. Such a localization of the drug could induce a local curvature and enlarges the space between the adjacent alkyl chains. This could allow the tails of the alkyl chains of the next layer to entangle, introducing tail interdigitation. Candesartan at low concentrations affects only the headgroup, probably spanning between the water interface and headgroup region. This may be attributed to attractive electrostatic interactions between the two anions of candesartan and the positively charged nitrogen of the choline group and repulsive interactions with the phosphate group, thus leading to its higher affinity to aggregate with the water interface as it adopts a more accessible area to hydrophilic environment. At higher concentrations, candesartan strengthens the polar interactions and also affects the packing of the alkyl chains, probably due to partial penetration into the hydrocarbon region.

Formation of Domains in the Lipid Bilayers. The most prominent effect of losartan in contrast to candesartan is the formation of different domains in the lipid bilayers, as noticed by the main transition asymmetric endothermic peak at high drug concentration. This phase separation induced by losartan is probably attributed to drug-poor and -rich domains in the lipid matrix. It has already been observed[47] by applying ESR spectroscopy that losartan at high concentrations inserts deeper into the DPPC bilayers, possibly due to the self-association of losartan molecules. The AT$_1$ antagonist valsartan displayed similar behavior with losartan, as reported in a very recent study. At 20 mol % valsartan incorporated in DPPC bilayers, the thermal scan shows a two component endothermic transition profile attributed to valsartan rich and pure domains.[29] On the other hand, experimental results show that candesartan partitions in a lower degree in the neutral DPPC bilayers compared with losartan. The heterogeneity of losartan's partition in the bilayer leads to the

J

dx.doi.org/10.1021/jp110371k |*J. Phys. Chem. B* XXXX, XXX, 000–000

creation of assemblies that could affect negatively the diffusion rate. It is more and more evident that drugs affect the lipid core and form microdomains in a different manner.

Bilayer Perturbation. Raman and DSC results suggested perturbation in the fluidity of the bilayer in both the gel and liquid crystalline phase with the intercalation of the sartan molecules. Candesartan, as DSC and Raman spectroscopy clearly showed, exerts milder thermal effects compared to losartan. In fact, the different pharmacological profiles of GPCR bioactive drugs have been associated with the perturbations they induce to membrane fluidity.[57]

The ratio $I_{2935/2880}$ regarding inter- and intrachain mobility indicates more pronounced effects with the presence of candesartan. The drastic lowering of the ratio $I_{2935/2880}$ should be attributed to an induced increased order at the bilayer surface, since the peak at 2880 cm^{-1} is indicative of the intermolecular order (intermolecular lateral packing and intramolecular conformational).[54] The DSC results complemented these findings, indicating that candesartan affects mainly the polar head region.

This increased order compared with losartan suggests a link between the structure rigidity and the effectiveness in the anchoring at the polar head region and packing between the alkyl chains. An identical relationship between GPCR cannabinoid agonists that act on the headgroup vicinity was recently reported by using solid state ^{2}H NMR spectroscopy. More specifically, the more rigid Δ^{8}-tetrahydrocannabinol compared with CP-55940 (synthesized by Pfizer) and WIN-55212-2 (discovered by the Sterling Winthrop research team) increased to a greater degree the order parameter of the bilayer core.[58]

The notable similarity between losartan/lipid interactions compared with the corresponding interactions of the potent antagonist valsartan as very recently presented[29] reinforces the suggested relationship. In particular, losartan possesses a butyl alkyl chain and valsartan a pentanamido butanoic acid segment, both characterized by high flexibility, as shown in our previous publications.[27,59,60]

In contrast, candesartan bears only a 2-ethoxy group which has limited flexibility. In addition, the heterocyclic part differs in the three molecules. Candesartan contains the very rigid 1,3-benzodiazole-6-carboxylic acid segment; losartan, the substituted imidazole ring at the 4 and 5 positions with chloro and $-CH_2OH$, respectively; and valsartan bears no heterocyclic ring.

The homogeneous broadening parameter brd confirmed in conjunction with the Raman observed ΔI changes of the 2935/2880 intensity ratio that the presence of sartans restrict the mobility of the alkyl chain. Furthermore, in accordance with DSC thermograms, the different phases are preserved in the presence of candesartan, whereas the pretransition is abolished with losartan.

Simulation of Drug/Membrane Interactions. The temperature profiles of the fitted parameters for the two bilayer samples (drug-free DPPC or DPPC/sartan bilayers) were directly compared with each other, and the fluctuations in the values of the parameters were related to the conformation and dynamics of the bilayers, reflecting differences in the dipolar ^{1}H$-^{31}$P interactions of the losartan and the candesartan with the bilayers.

The anisotropy of the CS tensor was used for the fitting of the ^{31}P NMR spectra. The principal elements of the shielding tensor of the DPPC lipid as derived from various levels of theory (Table 5) were used as initial input values to the simulation algorithm. Experimental spectra were simulated as described in ref 28, but the downhill simplex algorithm failed to give a satisfactory convergence. In contrast, a successful convergence at the preset criterion

was achieved when using as initial values the reported data for hydrated DPPC dispersions obtained at -110 °C.[55]

■ CONCLUSIONS

This research activity is a continuation of previous work and investigates the interactions of DPPC with incorporated sartan molecules by implementing DSC, solid state NMR, and Raman spectrosopic methods.[28] To the best of our knowledge, the ab initio implementation in a ^{31}P NMR fitting methodology constitutes a novel approach to further elucidate the drug/membrane interactions. The rationale for studying AT$_1$ antagonist/membrane interactions is that amphiphilic molecules may approach the receptor not through extracellular loops, but rather, by incorporating into the lipid core. This is in accordance with recent data obtained by Tomohiro et al. for the cannabinoid ligand CP.[61] Hitherto, such studies show that AT$_1$ antagonists do not exert a unique perturbing effect, but depend on the lipid matrix and the specific features of the studied molecule,[1,2,28,47,48] and hence, these results call for more comprehensive understanding of the role of lipid bilayers in the drug action to elicit information for their pharmacological activity. In fact, the significance of drug/membrane interactions in the medicinal chemistry field is outlined in a recent review publication.[62]

The combination of the three biophysical methods—DSC, Raman, and ^{31}P NMR broadline simulation methodology—revealed the different effects of the two sartan molecules on the lipids at the molecular level, confirming that each bioactive molecule has its special fingerprint when it interacts with membrane bilayers. Candesartan compared with losartan exhibited a different fluidizing effect, a different localization, and probably a different diffusion rate into the medium. This was based on (i) the homogeneous distribution of candesartan in the DPPC bilayer, in contrast to the inhomogenous distribution of losartan; (ii) the stronger polar interface activity of losartan; and (iii) the stronger inhibition in the mobility of the hydrophobic alkyl chains, especially in the liquid crystalline by candesartan.

The obtained results could suggest a relationship between the diffusion efficacy and the pharmacological potency of the studied sartan agents. Thus, losartan's tendency to form domains in the lipid bilayers could presumably retard its diffusion toward the active site of the AT$_1$ receptor. In addition, the diffusion may be retarded by its stronger binding to the headgroup region as well as the induction of the interdigitation effect. On the other hand, candesartan at higher concentration is not inhibited by such effects toward its diffusion trip at the AT$_1$ receptor. Its membrane perturbation effects are milder, and in contrast to losartan, its incorporation does not induce interdigitation to the lipid matrix.

It should be noted that the results from model membranes cannot be so easily extrapolated to describe the interaction of the studied AT$_1$ antagonists with natural membranes and trace the different pharmacological fingerprint of two antagonists. The observed differences, however, might relate to the differentiated pharmacological profile of the two studied AT$_1$ antagonists and plausibly in part explain the more potent profile of candesartan.

Therefore, the candesartan/membrane interactions could prove as useful insight in the design of novel molecules. The application of future rational drug design should also include drug/membrane interactions apart from the binding modes of the ligand in the receptor active site. This postulates the modulation of the vicinity proteins, and this observation may offer a new avenue in membrane lipid therapy.[57,63]

K

dx.doi.org/10.1021/jp110371k |J. Phys. Chem. B XXXX, XXX, 000–000

■ ASSOCIATED CONTENT

■ AUTHOR INFORMATION

Corresponding Author
*Phone: +30 210 7273870. Fax: +30 210 7273831. E-mail: mzervou@eie.gr.

■ ACKNOWLEDGMENT

■ REFERENCES

(1) Gasparo, M. D.; Catt, K. J.; Inagami, T.; Wright, J. W.; Ugner, T. *Pharmacol. Rev.* **2000**, *52*, 415–472.

(2) Wagenaar, L. J.; Voors, A. A.; Buikema, H.; van Buiten, A.; Lübeck, R. H.; Boonstra, P. W.; van Veldhuisen, D. J.; van Gilst, W. H. *Cardiovasc. Drugs Ther.* **2002**, *16*, 311–316.

(3) Unger, T. *Eur. Heart J. Suppl.* **2004**, *6*, H11–H16.

(4) Morsing, P.; Vauquelin, G. *Cell. Biochem. Biophys.* **2001**, *35*, 89–102.

(5) Zou, Y.; Akazawa, H.; Qin, Y.; Sano, M.; Takano, H.; Minamino, T.; Makita, N.; Iwanaga, K.; Zhu, W.; Kudoh, S.; Toko, H.; Tamura, K.; Kihara, M.; Nagai, T.; Fukamizu, A.; Umemura, S.; Iiri, T.; Fujita, T.; Komuro, I. *Nat. Cell Biol.* **2004**, *6*, 499–506.

(6) Yasuda, N.; Miura, S.; Akazawa, H.; Tanaka, T.; Qin, Y.; Kiya, Y.; Imaizumi, S.; Fujino, M.; Ito, K.; Zou, Y.; Fukuhara, S.; Kunimoto, S.; Fukuzaki, K.; Sato, T.; Ge, J.; Mochizuki, N.; Nakaya, H.; Saku, K.; Komuro, I. *EMBO Rep.* **2008**, *9*, 179–186.

(7) Zoumpoulakis, P.; Daliani, I.; Zervou, M.; Kyrikou, I.; Lamprinidis, G.; Mikros, E.; Mavromoustakos, T. *Chem. Phys. Lipids* **2003**, *125*, 13–25.

(8) Vauquelin, G.; Packeu, A. *Mol. Cell. Endocrinol.* **2009**, *311*, 1–10.

(9) Rumiana, K.; Caffrey, M. *Biochim. Biophys. Acta* **1998**, *1376*, 91–145.

(10) Tristram-Nagle, S.; Wiener, M. C.; Yang, C. P.; Nagle, J. F. *Biochemistry* **1987**, *26*, 4288–4294.

(11) Houslay, M. D. Stanley, K. K. *Dynamics of Biological Membranes*; John Wiley & Sons: New York, 1982.

(12) Rand, R. P.; Chapman, D.; Larsson, K. *J. Biophys.* **1975**, *15*, 1117–1124.

(13) Stamatoff, J.; Feuer, B.; Guggenheim, H. J.; Tellez, G.; Yamane, T. *J. Biophys.* **1982**, *38*, 217–226.

(14) McIntosh, T. J. *J. Biophys.* **1980**, *29*, 237–246.

(15) Colthup, N. B.; Daly, L. H.; Wiberley, S. E. *Introduction to Infrared and Raman Spectroscopy*; Academic Press: New York, 1990.

(16) Huang, C.; Lapides, J. R.; Levin, I. W. *J. Am. Chem. Soc.* **1982**, *104*, 5926–5930.

(17) Levin, I. W.; Lewis, E. N. *Anal. Chem.* **1990**, *62*, 1101A–1111A.

(18) Pabst, G.; Rappolt, M.; Amenitsch, H.; Laggner, P. *Phys. Rev. E* **2000**, *62*, 4000–4009.

(19) Silvius, J. R.; Lyons, M.; Yeagle, P. L.; O'Leary, T. J. *Biochemistry* **1985**, *24*, 5388–5395.

(20) Netticadan, T. J.; Ashavaid, T. F.; Nair, K. G. *Indian J. Clin. Biochem.* **1997**, *12*, 49–54.

(21) Theodoropoulou, E.; Mavromoustakos, T.; Panagiotopoulos, D.; Matsoukas, J.; Smith, J. *Lett. Pept. Sci.* **1996**, *3*, 209–216.

(22) Matsoukas, J. M.; Agelis, G.; Wahhab, A.; Hondrelis, J.; Panagiotopoulos, D.; Yamdagni, R.; Wu, Q.; Mavromoustakos, T.; Maia, H. L. S.; Ganter, R.; Moore, G. J. *J. Med. Chem.* **1995**, *38*, 4660–4669.

(23) Zoumpoulakis, P.; Zoga, A.; Roumelioti, P.; Giatas, N.; Grdadolnik, S. G.; Iliodromitis, E.; Vlahakos, D.; Kremastinos, D.; Matsoukas, J.; Mavromoustakos, T. *J. Pharm. Biomed. Anal.* **2003**, *31*, 833–844.

(24) (a) Moutevelis-Minakakis, P.; Gianni, M.; Stougiannou, H.; Zoumpoulakis, P.; Zoga, A.; Vlahakos, A. D.; Iliodromitis, E.; Mavromoustakos, T. *Bioorg. Med. Chem. Lett.* **2003**, *13*, 1737–1740. (b) Mavromoustakos, T.; Moutevelis-Minakakis, P.; Kokotos, C. G.; Kontogianni, P.; Politi, A.; Zoumpoulakis, P.; Findlay, J.; Cox, A.; Balmforth, A.; Zoga, A.; Iliodromitis, E. *Bioorg. Med. Chem.* **2006**, *14*, 4353–4360.

(25) Zoumpoulakis, P.; Politi, A.; Grdadolnik, S. G.; Matsoukas, J.; Mavromoustakos, T. *J. Pharm. Biomed. Anal.* **2006**, *40*, 1097–1104.

(26) Mavromoustakos, T.; Apostolopoulos, V.; Matsoukas, J. *Med. Chem.* **2001**, *1*, 207–217.

(27) Mavromoustakos, T.; Zervou, M.; Zoumpoulakis, P.; Kyrikou, I.; Benetis, N. P.; Polevaya, L.; Roumelioti, P.; Giatas, N.; Zoga, A.; Moutevelis Minakakis, P.; Kolocouris, A.; Vlahakos, D.; Grdadolnik, S. G.; Matsoukas, J. *Curr. Top. Med. Chem.* **2004**, *4*, 385–401.

(28) Fotakis, C.; Christodouleas, D.; Chatzigeorgiou, P.; Zervou, M.; Benetis, N. P.; Viras, K.; M. Mavromoustakos, T. *Biophys. J.* **2009**, *96*, 2227–2236.

(29) Potamitis, C.; Chatzigeorgiou, P.; Siapi, E.; Viras, K.; Mavromoustakos, T.; Hodzic, A.; Pabst, G.; Cacho-Nerin, F.; Laggner, P.; Rappolt, M. *Biochim. Biophys. Acta* **2011**, DOI: 10.1016/j.bbamem.2011.02.002

(30) Dasgupta, C.; Zhang, L. *Drug Discovery Today* **2011**, *16*, 22–34.

(31) Naik, P.; Murumkar, P.; Giridha, R.; Yadav, M. R. *Bioorg. Med. Chem.* **2010**, *18*, 8418–8456.

(32) Kyrikou, I.; Poulos, C.; Benetis, N.; Viras, K.; Zervou, M.; Mavromoustakos, T. *Biochim. Biophys. Acta* **2008**, *1778*, 113–124.

(33) *MacroModel, version 9.8*; Schrödinger, LLC: New York, NY, 2010.

(34) Jorgensen, W. L.; Tirado-Rives, J. *Proc. Natl. Acad. Sci. U.S.A.* **2005**, *102*, 6665–6670.

(35) *QikProp, version 3.3*; Schrödinger, LLC: New York, NY, 2010.

(36) Becke, A. D. *J. Chem. Phys.* **1993**, *98*, 5648–5652.

(37) Lee, C.; Yang, W.; Parr, R. G. *Phys. Rev. B* **1988**, *37*, 785–789.

(38) Krishnan, R.; Binkley, J. S.; Seeger, R.; Pople, J. A. *J. Chem. Phys.* **1980**, *72*, 650–654.

(39) Moller, C.; Plesset, M. S. *Phys. Rev.* **1934**, *46*, 618–622.

(40) Kutzelnigg, W. *Isr. J. Chem.* **1980**, *19*, 193–199.

(41) Schindler, M.; Kutzelnigg, W. *J. Chem. Phys.* **1982**, *76*, 1919–1933.

(42) Frisch, M. J.; Trucks, G. W.; Schlegel, H. B.; Scuseria, G. E.; Robb, M. A.; Cheeseman, J. R.; Zakrzewski, V. G.; Montgomery , J. A., Jr.; Stratmann, J. R. E.; Burant, C.; Dapprich, S.; Millam, J. M.; Daniels, A. D.; Kudin, K. N.; Strain, M. C.; Farkas, O.; Tomasi, J.; Barone, V.; Cossi, M.; Cammi, R.; Mennucci, B.; Pomelli, C.; Adamo, C.; Clifford, S.; Ochterski, J.; Petersson, G. A.; Ayala, P. Y.; Cui, Q.; Morokuma, K.; Malick, D. K.; Rabuck, A. D.; Raghavachari, K.; Foresman, J. B.; Cioslowski, J.; Ortiz, J. V.; Baboul, A. G.; Stefanov, B. B.; Liu, G.; Liashenko, A.; Piskorz, P.; Komaromi, I.; Gomperts, R.; Martin, R. L.; Fox, D. J.; Keith, T.; Al-Laham, M. A.; Peng, C. Y.; Nanayakkara, A.; Challacombe, M.; Gill, P. M. W.; Johnson, B.; Chen, W.; Wong, M. W.; Andres, J. L.; Gonzalez, C.; Head-Gordon, M.; Replogle, E. S.; Pople, J. A. *Gaussian 98, Revision A.9*; Gaussian, Inc.: Pittsburgh PA, 1998.

(43) Anet, F. A. L.; O'Leary, D. J. *Concepts Magn. Reson.* **1991**, *3*, 193–214.

(44) Soteriadou, K. P.; Tzinia, K. P.; Panou-Pomonis, A. K.; Tsikaris, V.; Sakarellos-Daitsiotis, M.; Sakarellos, C.; Papapoulou, Y.; Matsas, R. *Biochem. J.* **1996**, *313*, 455–466.

(45) Zoumpoulakis, P.; Grdadolnik, S. G.; Matsoukas, J.; Mavromoustakos, T. *J. Pharm. Biomed. Anal.* **2002**, *28*, 125–135.

(46) Kyonova, R.; Caffrey, M. *Biochim. Biophys. Acta* **1998**, *1376*, 91–145.

L

dx.doi.org/10.1021/jp110371k |*J. Phys. Chem. B* XXXX, XXX, 000–000

(47) Theodoropoulou, E.; Marsh, D. *Biochim. Biophys. Acta* **1999**, *1461*, 135–146.

(48) Theodoropoulou, E.; Marsh, D. *Biochim. Biophys. Acta* **2000**, *1509*, 346–360.

(49) Mavromoustakos, T.; Yang, D. P.; Makriyannis, A. *Biochim. Biophys. Acta* **1995**, *1239*, 257–264.

(50) Mavromoustakos, T.; Chatzigeorgiou, P.; Koukoulitsa, C.; Durdagi, S. *Int. J. Quantum Chem.* **2011**, *111*, 1172–1183.

(51) McMullen, T. P.; McElhaney, R. N. *Biochim. Biophys. Acta* **1995**, *1234*, 90–98.

(52) Vist, M. R.; Davis, J. H. *Biochemistry* **1990**, *29*, 451–464.

(53) O'Leary, T. J.; Ross, P. D.; Levin, I. W. *Biochemistry* **1984**, *23*, 4636–4641.

(54) O'Leary, T. J.; Levin, I. W. *Biochim. Biophys. Acta 776* **1984**, *776*, 185–189.

(55) Yeagle, P. L. *Biol. Magn. Reson.* **1990**, *9*, 153–155.

(56) Harrold, M. *Foye's Principles of Medicinal Chemistry*, 5th ed.; Williams, D. A., Lemke, T. L., Eds.; Lippincott Williams & Wilkins: Philadelphia, 2002.

(57) Lombardi, D.; Cuenoud, B.; Kramer, S. D. *Eur. J. Pharm. Sci.* **2009**, *38*, 533–547.

(58) Tian, X.; Pavlopoulos, S.; De-Ping, Y.; Makriyannis, A. *Biochim. Biophys. Acta* **2010**, doi:10.1016/j.bbamem.2010.11.026

(59) Mavromoustakos, T.; Kolocouris, A.; Zervou, M.; Roumelioti, P; Matsoukas, J.; Weisemann, R. *J. Med. Chem.* **1999**, *42*, 1714–1722.

(60) Potamitis, C.; Zervou, M.; Katsiaras, V.; Zoumpoulakis, P.; Durdagi, S.; Papadopoulos, M. G.; Hayes, J. M.; Grdadolnik-Golic, S.; Kyrikou, I.; Argyropoulos, D.; Vatougia, G.; Mavromoustakos, T. *J. Chem. Inf. Model.* **2009**, *49*, 726–739.

(61) Tomohiro, K.; Kejun, C.; Kenner, R. C.; Gawrisch, K. *Biophys. J.* **2009**, *96*, 4916–4924.

(62) Lucio, M; Lima, J. L. F. C.; Reis, S. *Curr. Med. Chem.* **2010**, *17*, 1795–1809.

(63) Ojima, M.; Inada, Y.; Shibouta, Y.; Wada, T.; Sanada, T.; Kubo, K.; Nishikawa, K. *Eur. J. Pharmacol.* **1997**, *319*, 137–146.